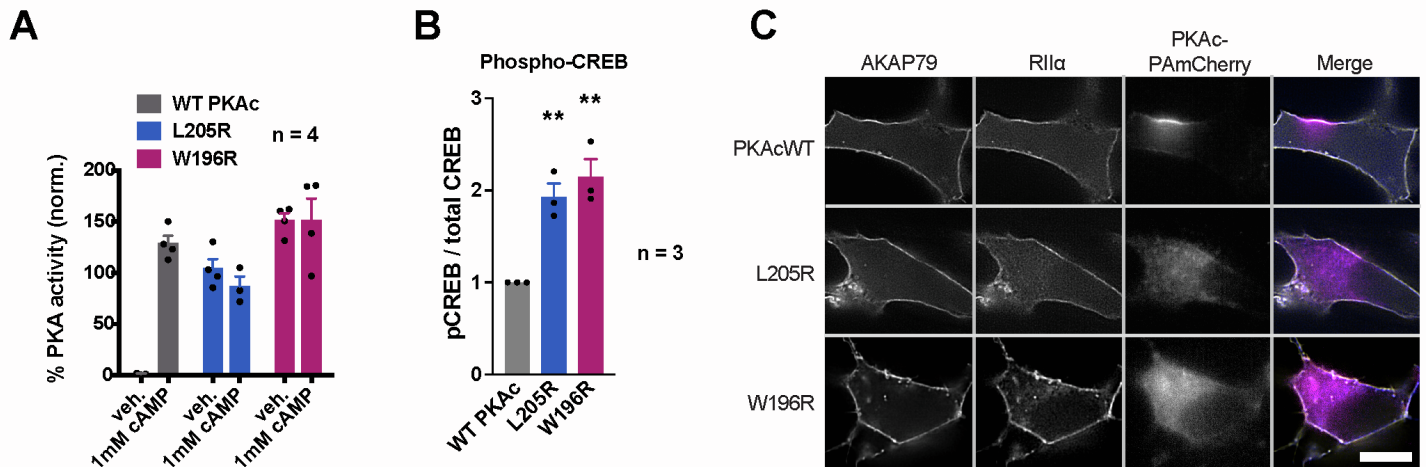


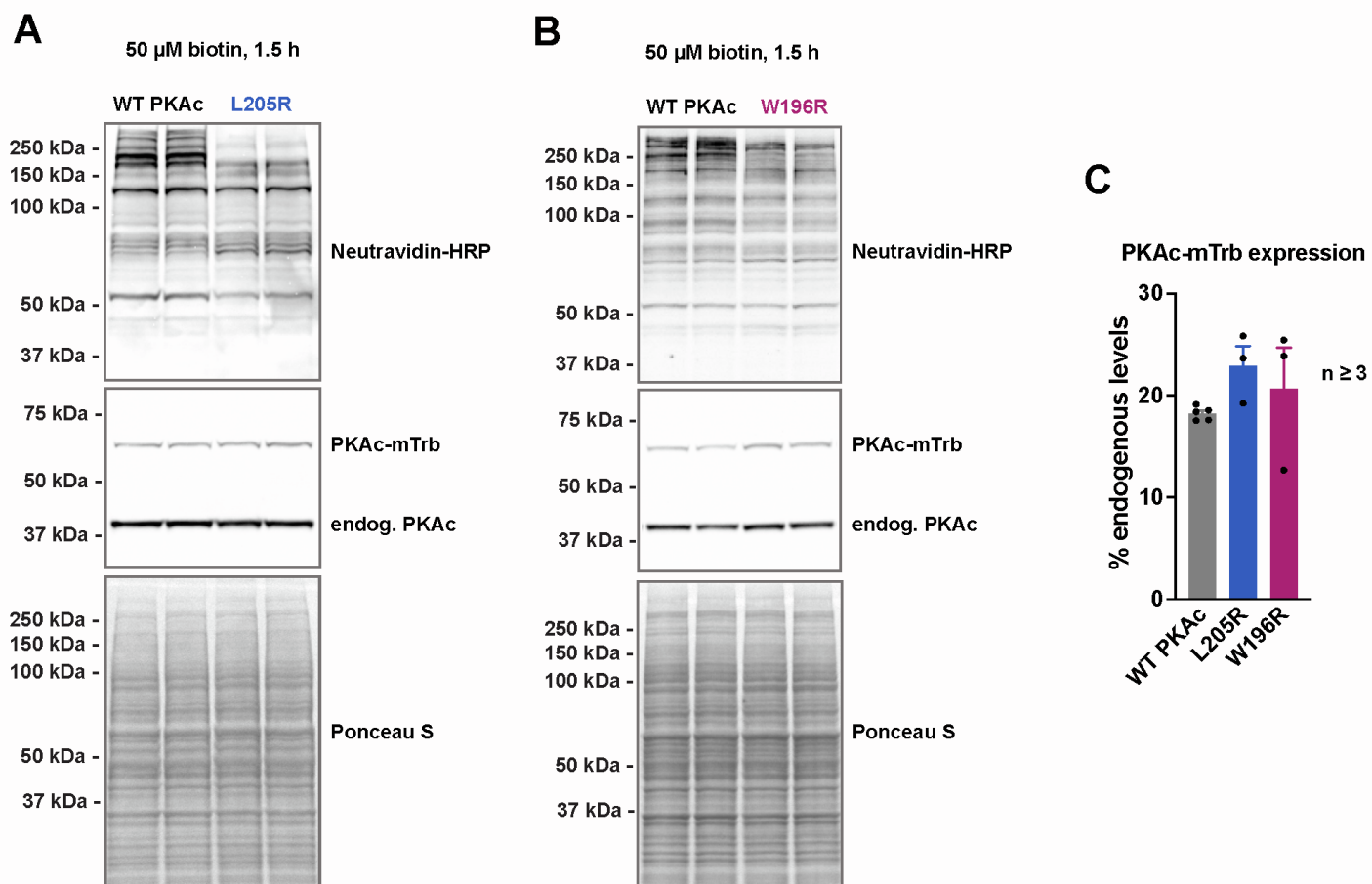
Supplemental information

**Mislocalization of protein kinase A drives
pathology in Cushing's syndrome**

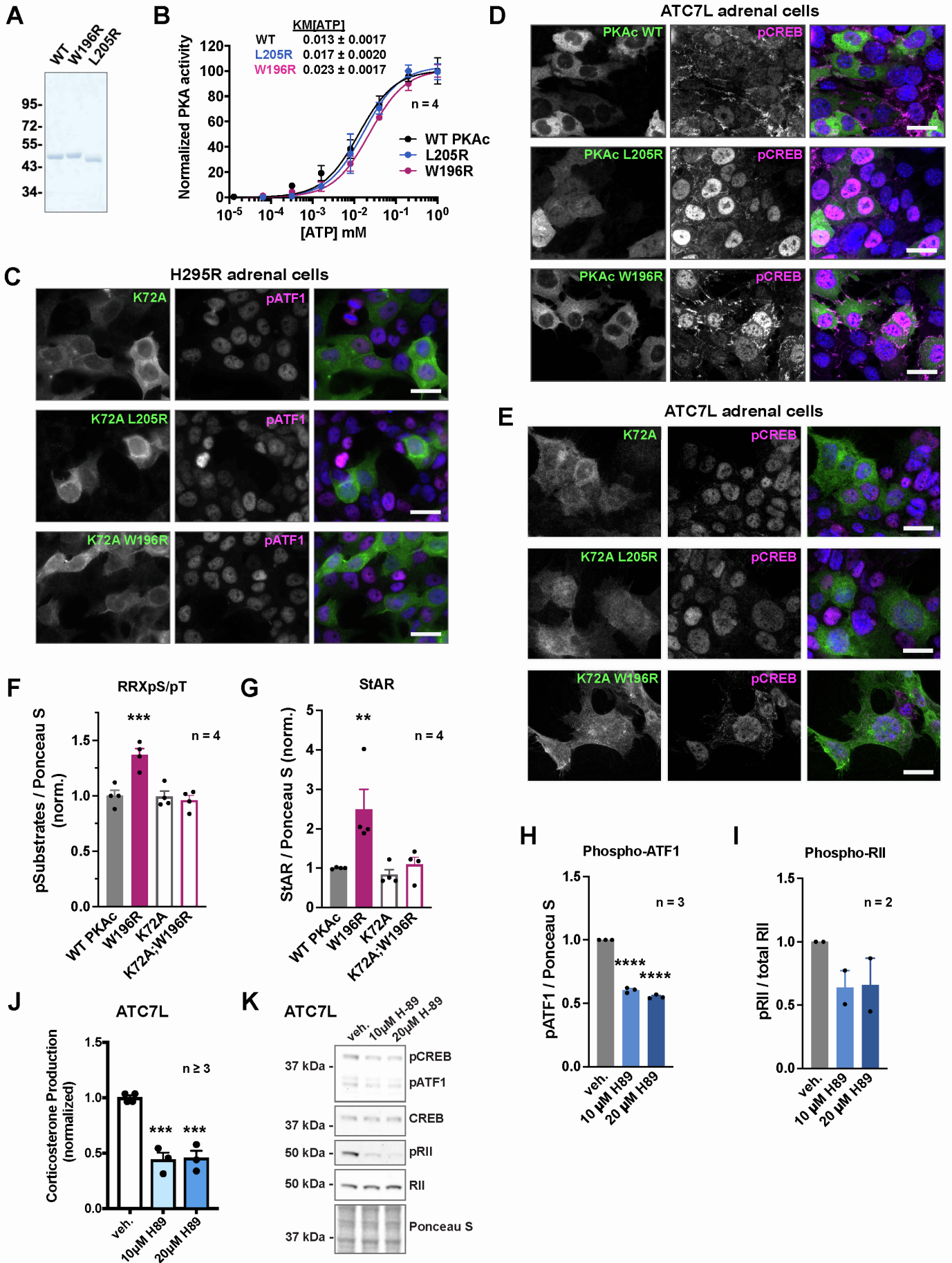
Mitchell H. Omar, Dominic P. Byrne, Kiana N. Jones, Tyler M. Lakey, Kerrie B. Collins, Kyung-Soon Lee, Leonard A. Daly, Katherine A. Forbush, Ho-Tak Lau, Martin Golkowski, G. Stanley McKnight, David T. Breault, Anne-Marie Lefrançois-Martinez, Antoine Martinez, Claire E. Eyers, Geoffrey S. Baird, Shao-En Ong, F. Donelson Smith, Patrick A. Eyers, and John D. Scott



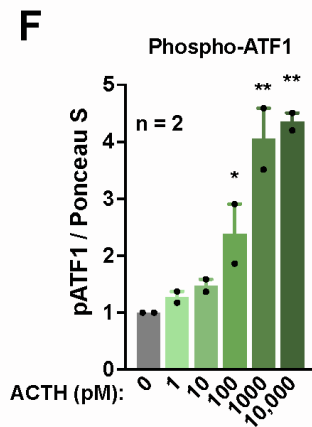
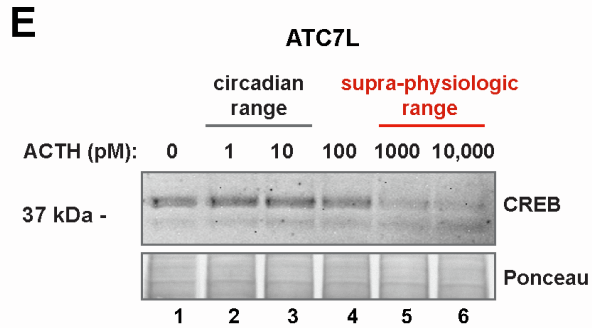
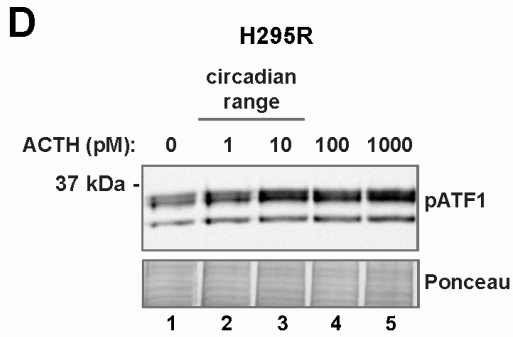
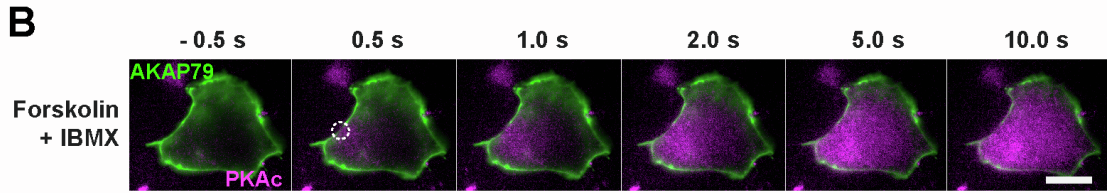
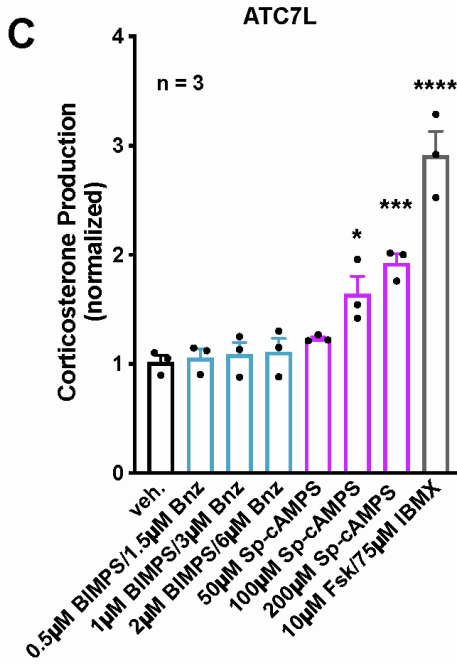
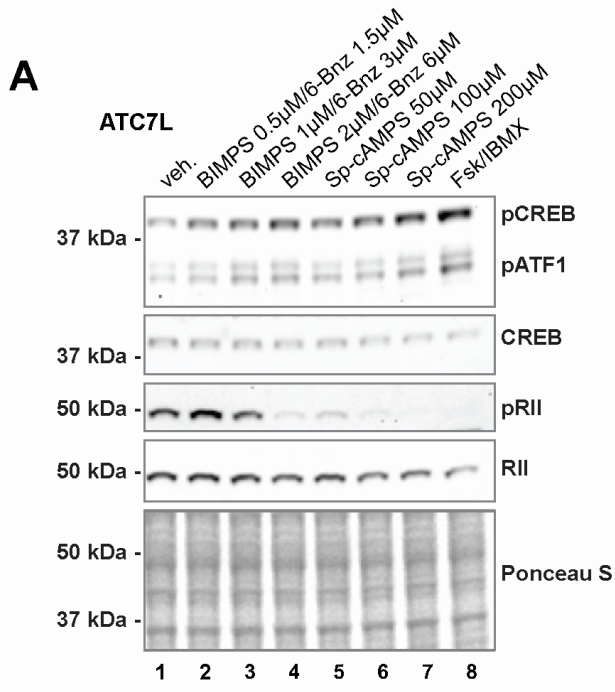
Supplemental figure S1. PKAc-L205R and PKAc-W196R are constitutively active and aberrantly mobile. Relates to figure 1. A) Activity of PKAc variants in the presence of RII +/- cAMP. n = 4. B) Quantitation from figure 1I of phospho-CREB divided by total CREB. ** $p < 0.01$, corrected for multiple comparisons with Holm-Sidak method after 1-way ANOVA. n = 3. C) 3-channel representative images of photoactivation cells demonstrating equivalent expression and colocalization of AKAP79 and RII. Scale bar = 10 μ m.



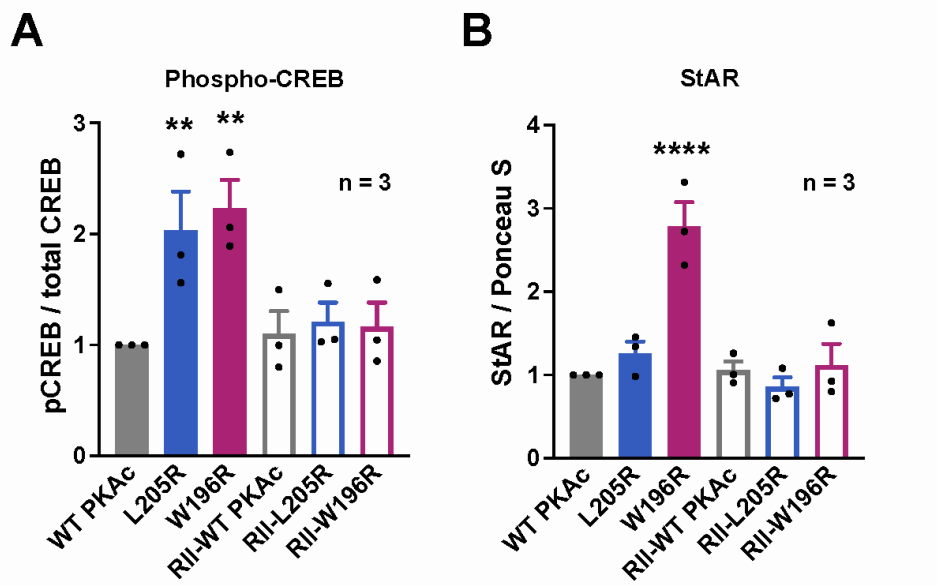
Supplemental figure S2. PKAc-miniTurbo variants are expressed at moderate levels and equally biotinylate proteins. Relates to figure 2. A & B) Representative western blots for L205R (A) and W196R (B) variants of PKAc-miniTurbo expressed in H295R cells and incubated with 50 μ M biotin for 1.5 h. C) Quantitation of PKAc-miniTurbo expression as compared to endogenous PKAc. No significant differences by 1-way ANOVA. n \geq 3.



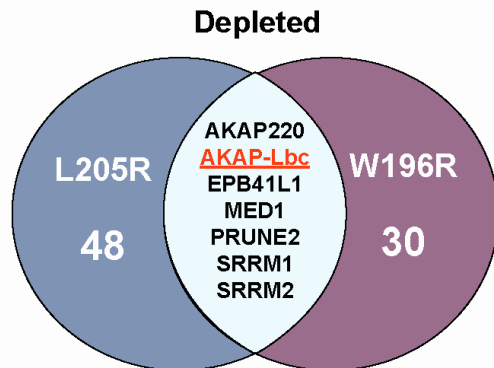
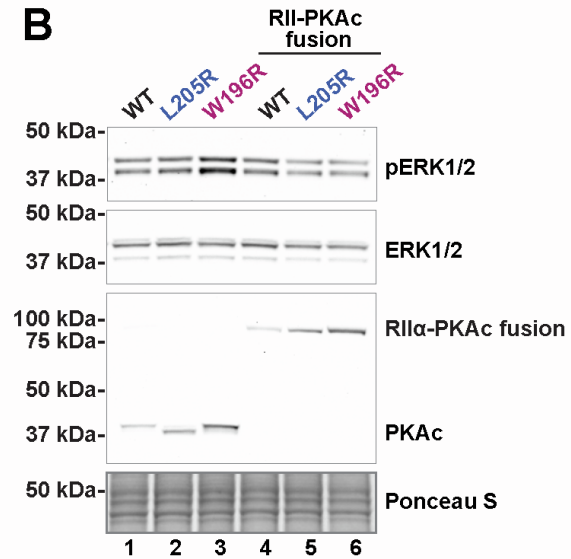
Supplemental figure S3. Cushing's mutants aberrantly phosphorylate substrates. Relates to figure 3. A) SDS-PAGE and Coomassie blue staining of purified recombinant WT and mutant PKAc variants. B) $K_M[ATP]$ determination for recombinant WT and mutant PKAc. Data shown is PKA-catalyzed peptide phosphorylation (pmol phosphate/min/ng protein) with increasing concentrations of ATP. Normalized to the maximum rate of phosphorylation for each protein. $K_M[ATP]$ values (\pm SE) were calculated from four independent experiments. C) H295R adrenal cells expressing kinase dead (K72A) versions of V5-tagged PKAc variants stained with V5 and pCREB antibodies. Scale bars = 20 μ m. D & E) ATC7L mouse adrenal cells expressing V5-tagged WT or mutant PKAc (D) or kinase dead (K72A) versions of these (E) were stained with V5 and pCREB antibodies. Scale bars = 20 μ m. F & G) Quantitation of phospho-RRXS/T (F) and StAR (G) immunoblots (figure 3H). ** $p \leq 0.01$, *** $p \leq 0.001$, corrected for multiple comparisons with Holm-Sidak method after 1-way ANOVA. $n = 4$. H & I) Quantitation of phospho-ATF1 (H) and phospho-RII (I) immunoblots (figure 3J). **** $p \leq 0.0001$, corrected for multiple comparisons with Holm-Sidak method after 1-way ANOVA. J) Corticosterone measurements from ATC7L cells after 1 h incubation with vehicle or the PKA inhibitor H89. *** p -value ≤ 0.001 . Corrected for multiple comparisons using Sidak method. $n \geq 3$. K) Immunoblot of ATC7L lysates after 1 h incubation with vehicle or H89. Representative of 3 experimental replicates.



Supplemental figure S4. Moderate activation does not displace PKAc-WT in adrenal cells. Relates to figure 4. A) Immunoblot of ATC7L lysates treated for 1 h with vehicle or increasing concentrations of PKA-activating drugs probed for pCREB/pATF1, total CREB, pRII, and RII. Representative of 3 experimental replicates. B) Photoactivation microscopy timecourse of H295R cell expressing AKAP79-YFP, RII-iRFP, and WT-PKAc tagged with photoactivatable mCherry in the presence of 10 μ M forskolin and 75 μ M IBMX. White circle indicates region of photoactivation. Scale bar = 10 μ m. C) Corticosterone measurements from ATC7L cells after 1 h with vehicle or increasing concentrations of PKA-activating drugs. n = 3. D) Representative immunoblot of H295R cells after treatment for 1 h with increasing concentrations of ACTH. E) Corresponds to figure 4K. Total CREB and Ponceau S immunoblot of ATC7L cells after treatment for 1 h with increasing concentrations of ACTH. F) Quantification of figure 4K phospho-ATF1 signal divided by Ponceau S. * $p < 0.05$, ** $p \leq 0.01$, corrected for multiple comparisons with Holm-Sidak after 1-way ANOVA. n = 2 full dosage curves.

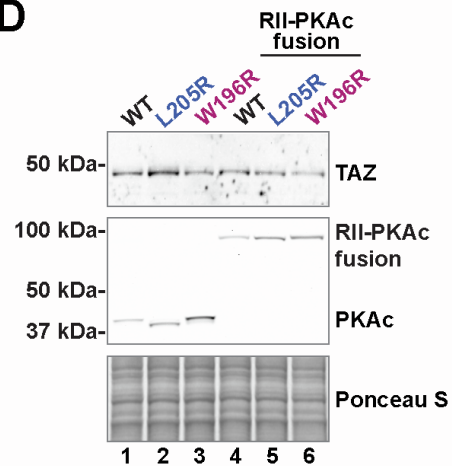


Supplemental figure S5. Fusion of Cushing's mutants to RII corrects stress hormone production. Relates to figure 5. Quantitation of immunoblots represented in figure 5F. ** $p \leq 0.01$, **** $p \leq 0.0001$, corrected for multiple comparisons with Holm-Sidak after 1-way ANOVA. $n = 3$.

A**B****C**

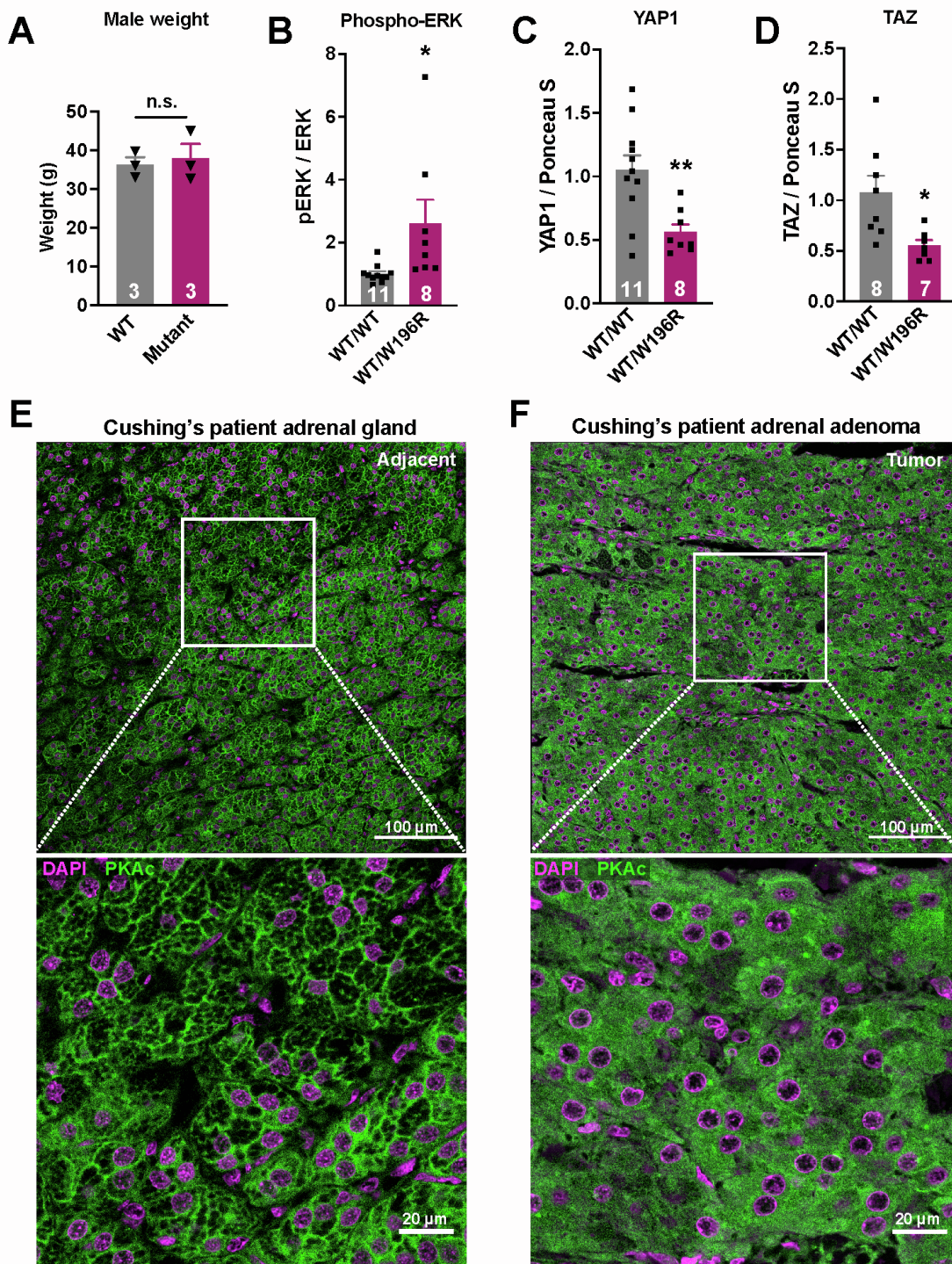
L205R proximity-labeled DLG5 phosphopeptides

S295 GDLRAQQQVLKHNGSSEILNKLYDTAMDKL
S1263 ATHGSNSLPSSARLGSSSNLQFKAERIKIPS
S1666 IPSKYVMDQEFSRRLSMSEVKDDNSATKTLS

D

Supplemental figure S6. Proximity phosphoproteomics identifies aberrant signaling by PKAc mutants.

Relates to figure 6. A) Venn diagram of significantly depleted phosphopeptides in both mutant conditions. B) Immunoblot of ATC7L cells lysates. Conditions expressing separate RII and PKAc proteins demonstrated increased ERK phosphorylation in the W196R condition. This effect was rescued by fusion of RII and PKAc. C) Discs large 5 phosphopeptides identified in PKAc-L205R proximity phosphoproteomic screen. Red indicates the phosphorylated residue. Underlined region is a conforming PKA substrate recognition motif. D) Immunoblot of ATC7L cells expressing separate (lanes 1-3) or fused (lanes 4-6) RII and PKAc variants.



Supplemental figure S7. A Cushing's mouse model and patient tissue display signaling defects. Relates to figure 7. A) Weight of 1-year male mutant mice (red) compared to littermate controls (gray); n = 3. Not significantly different by students t-test. B-D) Corresponds to figure 7J. Quantitation of adrenal gland immunoblot signals from multiple mice. *p<0.05, **p<0.01, students t-test. n \geq 7 mice. E & F) Immunofluorescence in resected tissue from an additional Cushing's patient. PKAc (green) and DAPI (magenta) were stained in normal adjacent adrenal tissue (E) and adenoma (F). Scale bars as indicated.